

Received: 11 March 2021 • Accepted: 21 May 2021

Research

doi: 10.22034/JCEMA.2021.281967.1055

Comparison of Quasi-Static and Dynamic Stress-Strain Analysis in Earth Dams (Case Study: Azadi Earth Dam)

Behrang Beiranvand*, Mostafa Zeinolebadi Rozbahani, Ahmadreza Mazaheri

Department of Water Engineering and Hydraulic Structures, University of Ayatollah Ozma Borujerdi, Lorestan, Iran.

* Correspondence should be addressed to Behrang Beiranvand, Department of Water Engineering and Hydraulic Structures, University of Ayatollah Ozma Borujerdi, Lorestan, Iran. Tel: +986633231711, Email: behrang220@gmail.com.

ABSTRACT

Seismic analysis of earth and rockfill dams is generally done in two ways: quasi-static and dynamic. However, a quasi-static method with easy application and simple assumptions may lead to unsafe and uneconomical results. In the present study, two static and dynamic analyzes have been used nonlinearly using the Rayleigh Damping rule to calculate the stress and strain of Azadi Dam in the stages of the end of construction and steady-state seepage. Also, in numerical analysis, Abaqus software and a simple elastoplastic behavior model based on the Mohr-Coulomb criterion have been used. The results show that in both quasi-static and dynamic seismic analysis, the highest strain of the Azadi Dam core occurred at the upper levels of the core and the highest stress occurred at the level of the core floor. The stress in the dynamic state is higher than the quasi-static one in the directions σ_{xx} 49%, σ_{xy} 30%, and σ_{yy} 28%, respectively. Also, the maximum shell stress at 1255 m, 1275 m, and 1300 m levels is 29%, 68%, and 72% higher than the core,

Keywords: Abaqus, quasi-static analysis, dynamic analysis, stress, strain

Copyright © 2021 Behrang Beiranvand. This is an open access paper distributed under the [Creative Commons Attribution License](https://creativecommons.org/licenses/by/4.0/). *Journal of Civil Engineering and Materials Application* is published by [Pendar Pub](https://www.pendarpub.com/); Journal p-ISSN 2676-332X; Journal e-ISSN 2588-2880.

1. INTRODUCTION

Seismic design and analysis of earth and rockfill dams are done by two methods, quasi-static and dynamic. The method of dynamic analysis is mainly based on stress analysis and displacement, which is usually done with the help of finite element methods. This method is commonly used to analyze the stability of large dams in the study phase. Lack of accurate software for dynamic analysis of earth dams, the limited number of experts aware of dynamic analysis, the complexity of dynamic analysis method, expensive tests for determining dynamic soil properties, frequency, and ease of analysis with quasi-static software are the reasons for widespread use of the quasi-static method. Due to these cases, determining the accuracy of the quasi-static method and creating a relationship between the solutions of the two quasi-static and dynamic methods is of interest to earth and gravel dam design engineers. Today, the development of finite element and finite difference software has made it possible to use dynamic analysis as well as quasi-static analysis. Ambraseys and Sarma, 1967 examined the

response of earth dams to several earthquakes. They calculated the time history and distribution of earthquake acceleration in the dam body [1]. (Sarma, 1975) developed diagrams for calculating the critical horizontal acceleration in which the critical horizontal acceleration is the acceleration that can bring the soil mass limited to a landslide level into equilibrium [2]. (Wang et al., 2006) introduced a new model in FLAC software and dynamically analyzed several earth dams in the effective stress space. They compared the actual deformations of the dams with the estimated values with different models [3]. (Tsai et al., 2006) by studying the dynamic response of the Pao-Shan dam, studied the effect of core dimensions on the potential of earth dam response as well as the effect of core width and height ratio and dam length and height ratio at the first natural frequency [4]. (Tsompanakis et al., 2009) Using a neural network, evaluated the dynamic response of the sample embankment (laboratory) using the finite element method. Considering the nonlinear behavior of soil materials, he concluded that the magnification

module would shrink as the maximum earthquake acceleration increases and the materials enter the nonlinear section [5]. (Elia et al., 2011), investigated the seismic and aftershock behavior of the Marana homogeneous dam in Italy [6]. (Mukherjee, 2013) The basic concepts of different methods of seismic stability analysis of earth dams and salient features, advantages, and limitations of each. To realistically predict the earth dam response during an earthquake, the factors of nonlinear soil elastic behavior, the dependence of the enclosed soil pressure on its stiffness, the geometry of the valley, and the intersection of the dam with the alluvium must be carefully considered [7]. (Huang, 2014) analyzed the seismic response of earth dams with stabilizing materials (materials with low strength control, CLSM) using the finite element method. Their results show that the use of CLSM is suitable for stabilizing embankments against seismic excitation [8]. According to studies (Panulinova and Harabinova, 2014), the stability of earth dams against landslides or seismic effects should be designed so that the

embankment is not destroyed due to changes in soil properties or external influences and remains stable [9]. (Bandini et al., 2015) presented a limit equilibrium model in which changes in block geometry and changes in shear strength due to slip are considered. He compared the results of observational models with the results of numerical analysis [10]. In all these comparisons, the observed behavior is consistent with the predicted one, which indicates the need to consider the block geometry change and the shear strength due to shear in the calculations. In this study, quasi-static and dynamic analysis of stress-strain in the Azadi earth dam after the end of the construction phase and in the steady-state seepage using Abaqus software and nonlinear analysis have been investigated and compared. Finally, the degree of conformity with the percentages presented in the stress-strain analysis at different levels of the body and core of Azadi Dam, as well as the difference between quasi-static and dynamic methods, are shown.

2. MATERIALS AND METHODS

2.1. GEOGRAPHICAL LOCATION AND GEOLOGY OF AZADI DAM

Azadi Reservoir Dam is located in Iran and Kermanshah province, 500 m downstream of Shahgozar Bridge, and about 90 km from Javanrood city in the coordinates of 46°21 east longitude, and 34°33 north latitude on Zamkan River. The catchment area of this river up to the axis of Azadi Dam is 1054 km². Access to Azadi Reservoir Dam

is possible through Kermanshah Road, Kuzran-Shahgozar Bridge. Azadi Dam is a rockfill type with a clay core with a height of 64 m from the foundation to 1312 (masl) meters above sea level and a crest length of 737 m. The volume of the dam reservoir at the normal level is 57.47 million m³ and the useful volume is 50 million m³ (Figure 1).

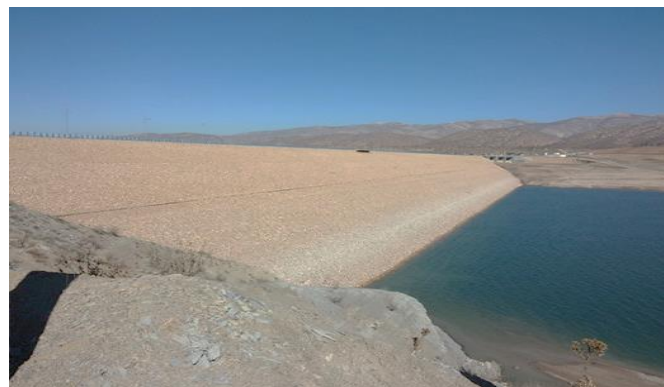


Figure 1. Azadi earth dam, Kermanshah, Iran

Azadi Reservoir Dam site consists of two rocky sections of Chilean Amiran sediments and marl limestone of Gurpi Formation and the alluvial-debris sediment unit of the present period in the right-axis ridge and under the overflow. In terms of geostructure, the area of Azadi Dam and related facilities belong to the folded Zagros structural unit in East Lorestan. This structural unit, like other folded Zagros regions in the south and southwest of Iran, has a stressful past in terms of tectonic activity. Of course, in this area, folding and faulting of formations are normal and natural (Abdan Faraz Consulting Engineers). Azadi

Reservoir Dam site is composed of two rock sections: Amiran Formation shale sediments - Gurpi Formation marl limestone and alluvial-debris sediments of the present era in the right-axis and below the overflow. In terms of geostructure, the area of Azadi Dam and related facilities belong to the Zagros fold and thrust belt structural unit (Zagros FTB) in East Lorestan. This structural unit, like other Zagros FTB areas in the south and southwest of Iran, has had many tectonic activities in the past. Of course, in this area, the folds and faults of the formations are normal (Abdan Faraz Consulting Engineers) [11].

2.2. GOVERNING EQUATIONS FOR STRUCTURAL DYNAMICS

By discretizing the dynamic equation of the structure and considering the applied forces of the earthquake in the time domain, and using the finite element approach, the $[M]\{\ddot{U}^{\cdot\cdot}\} + [C]\{\dot{U}^{\cdot}\} + [K]\{U\} = \{F_{-1}\} - [M]\{U_{-g}\} + [Q]\{P\}$

dynamic equation governing the dam and foundation will be written in matrix form (1):

$$(1)$$

[M], [C], and [K] are the matrices of mass, damping, and stiffness of the structure, respectively. {U}, {U^ˆ}, {U^ˆ(..)}, {F₁} and {U_g} are the relocation, velocity, structural

acceleration, body forces, and earthquake acceleration, respectively.

2.2.1. Complete Elastoplastic Analysis of Embankment Assuming Mohr-Coulomb Theory

In an elastic-plastic analysis (complete plastic), the beginning of the stress-strain curve is linear, and its plastic range is linear. A yield function must be defined to evaluate whether the point has reached the plastic limit. Yield Criterion is usually expressed in terms of principal $F=f(\sigma_1, \sigma_2, \sigma_3, n_1, n_2, n_3)$

stresses or stress tensor variables. The onset of the condition is determined by the surrender criteria. The general form of the Yield Criterion can be given as Equation (2).

$$(2)$$

n_i show the direction of the main stresses σ_i . If the materials

are the same, the Yield Criterion becomes a simple equation (3):

$$F=f(\sigma_1, \sigma_2, \sigma_3)$$

$$(3)$$

If the stress field is such that $F(\sigma) < 0$ is the behavior of the elastic material, and as soon as the yield point $0 = F(\sigma)$ is reached, the plastic behavior of the material begins. In the

complete elastic model, the strain diagram consists of two components, elastic and plastic (Equation 4):

$$d\epsilon = [d\epsilon]^e + [d\epsilon]^p$$

$$(4)$$

For plastic strains, the law of flow is determined. The law of flow assumes that the plastic strain is perpendicular

to a plane. This law is defined as Equation (5):

$$[d\epsilon]^p = \lambda (\partial f(\sigma) / \partial \sigma^i)$$

$$(5)$$

Where λ is scalar and $f(\sigma)$ is a level of stress function. If $f(\sigma)$ is the same as the yield function, the related flow law holds. Otherwise, the law of flow will be unrelated, in

which case, in addition to defining the yield function, a new function $[g(\sigma)]$ will be defined, on which the plastic strain diagram will be perpendicular (Equation 6):

$$[d\epsilon]^p = \lambda (\partial g / \partial \sigma^i)$$

$$(6)$$

λ : is called the plastic coefficient, which in the elastic condition has a value of zero and in the plastic condition

will have a value greater than zero. The general relationship between the effective stress diagram and the strain diagram can be expressed as Equations (7) and (8):

$$\sigma^i = [D^e - \alpha/d D^e (\partial g / \partial \sigma^i) (\partial f^T) / (\partial \sigma^i)] D^e \epsilon^0$$

$$(7)$$

$$d = (\partial f^T) / (\partial \sigma^i) D^e (\partial g / \partial \sigma^i)$$

$$(8)$$

If the soil behavior is elastic, α is zero, and otherwise, α equals one. Also, f is the yield function and g is the plastic potential level. If the Mohr-Coulomb Yield Criterion is,

the Yield Criterion is defined as relations (9), (10), and (11):

$$f_1 = 1/2 |\sigma_2^i - \sigma_3^i| + 1/2 (\sigma_2^i + \sigma_3^i) \sin \phi - c \cos \phi \geq 0$$

$$(9)$$

$$f_2 = 1/2 |\sigma_3^i - \sigma_1^i| + 1/2 (\sigma_3^i + \sigma_1^i) \sin \phi - c \cos \phi \geq 0$$

$$(10)$$

$$f_3 = 1/2 |\sigma_1^i - \sigma_2^i| + 1/2 (\sigma_1^i + \sigma_2^i) \sin \phi - c \cos \phi \geq 0$$

$$(11)$$

The main parameters representing the Yield Criterion are the internal friction angle (ϕ) and soil cohesion (c), respectively. The shape of the function is conical in that the points inside it show the elastic range and the border

points show the plastic threshold. Since there is no related flow law in the Mohr-Coulomb Yield Criterion, the g function for the model is defined as a relation (12), (13) and (14):

$$g_1 = 1.2 |\sigma_2^i - \sigma_3^i| + 1.2 (\sigma_2^i + \sigma_3^i) \sin \psi$$

$$(12)$$

$$g_2 = 1.2 |\sigma_3^i - \sigma_1^i| + 1.2 (\sigma_3^i + \sigma_1^i) \sin \psi$$

$$(13)$$

$$g_3 = 1.2 |\sigma_1^i - \sigma_2^i| + 1.2 (\sigma_1^i + \sigma_2^i) \sin \psi$$

$$(14)$$

Parameter Ψ is used to model the volumetric strains of plastic in soils that increase in volume during cutting. Also, in the presence of cohesion, the Mohr-Coulomb model allows the element to be stretched, but in the modified

$$f_4 = \sigma_1 - \sigma_3 \geq 0 \tag{15}$$

$$f_5 = \sigma_2 - \sigma_3 \geq 0 \tag{16}$$

$$f_6 = \sigma_3 - \sigma_1 \geq 0 \tag{17}$$

At new levels, it is assumed that the related law is in place. If the stress range is within the yield function, the body behavior will be a function of the hook linear model. According to what has been said, in this model, the stress-strain relationship is defined by defining 5 parameters that can be achieved by known and common experiments in

Mohr-Coulomb Yield Model used in the program, the points under tension can be eliminated by defining complementary functions. These functions are defined as relations (15), (16), and (17):

soil. These parameters are soil shear modulus, Poisson's ratio, friction angle, cohesion, and expansion angle, which are formulated in equilibrium and compatibility equations in each of the elements by assuming planar strains and are determined by gradually applying loads and comparing them with yielding levels. (Zienkiewicz, et al., 1977) [11].

2.3. MODELING AZADI DAM IN ABACUS SOFTWARE

Abaqus is a set of highly powerful finite element modeling programs capable of solving simple to complex linear analysis and nonlinear modeling problems. In the nonlinear analysis, Abaqus automatically selects the values of the convergence tolerances and also adjusts their values during the analysis to obtain the correct answer. As a result, the user rarely has to specify the values of the numerical solution control parameters. It also supports Python open-source programming language for

programming within the software. The ability to write scripts in software doubles its modeling capabilities. In this research, Abaqus has been used to calculate the stress and strain pressure, assuming the flat strain behavior in Azadi Dam. For this purpose, the largest section of the dam has been modeled using Abaqus software and analyzed with eight-node elements [12]. Figure 2 shows the modeling and meshing of the Azadi Dam.

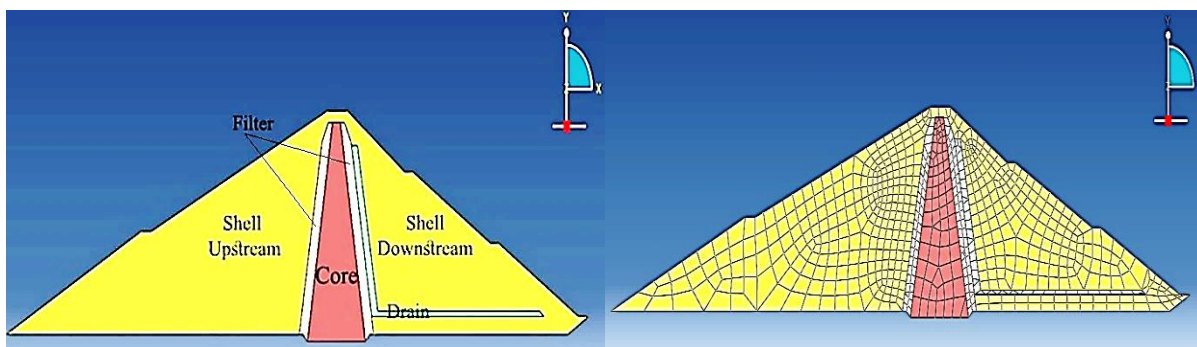


Figure 2. Modeling and meshing of Azadi Dam in Abacus software

For dynamic analysis, it is first necessary to perform quasi-static analysis and after equilibrium, dynamic analysis is started. The damping used in the dynamic analysis of the Azadi Dam is of the Rayleigh Damping type. Rayleigh Damping is the most common type of mechanical damping used in dynamic analysis. Rayleigh Damping is generally used in time-dependent applications to provide attenuation that is almost independent of frequency. Damping percentage is considered equal to 1% due to the elastoplasticity of the behavioral model of the materials. In behavioral models that allow the soil to enter the plastic part (Mohr-Coulomb), considering the energy dissipation capability in the model, it is reasonable to include damping between 0 and 1%. In fact, for most dynamic analyzes that involve large strain conditions, only a small percentage of damping is required. To evaluate the performance and seismic design of dams against earthquakes, the force caused by the earthquake should be suitably applied to the dam structure and the seismic responses of the dam should be calculated by performing nonlinear analysis. Since the Azadi Dam site is located on the Shale rock foundation, the location of the accelerometer must be consistent with the geological conditions of the site. Therefore, for the

dynamic analysis of Azadi Dam, the accelerometers of earthquakes have been selected that have been recorded on rocks or rocks with a shear velocity of less than 760 m/sec. It should be noted that the accelerometers have been selected based on the type of soil at the station (soil II). For this purpose, the soil of the stations in question has been determined based on geophysical methods. Based on seismicity studies in the area of the Azadi Dam construction site, the values of design basis seismicity parameters (DBL), design top (MDL), and maximum acceptability (MCL) are 0.20, 0.30, and 0.51, respectively, for maximum horizontal acceleration and 0.12, 0.20 and 0.34 were estimated for the maximum vertical acceleration and the maximum earthquake in the region with a magnitude of 7 (Abdan Faraz Consulting Engineers). In the study site, the earthquake coefficient has been determined and selected for stability analysis of 0.17 (equivalent to one-third of the maximum tolerated earthquake, based on Pyke's recommendation). Limiting the maximum acceleration of the input stimulus is 0.17 g due to the dynamic analysis of moderate and weak earthquakes by accepting low error and assuming linear soil behavior. It can also be related to the avoidance of

unrealistic tensile stresses in the lower shell elements, which occurred after adding dynamic to quasi-static stresses in earthquakes larger than 0.17 g due to the linear behavior assumption. Assuming the true nonlinear behavior of the soil and the inability to withstand the tensile strength of the aggregates, this problem can be

solved. Therefore, to perform dynamic analysis and generate the input stimulus, the Tabas earthquake accelerometers with a maximum acceleration of 0.83 g and 33 seconds have been used with the idea (Table 1 and Figure 3).

Table 1. Earthquake characteristics used in dynamic analysis of Azadi Dam

Earthquake	Maximum acceleration (g)	Maximum velocity (m/sec)	Maximum Horizontal displacement(m)	Time (sec)
Tabas	0.83	0.97	0.38	16.42

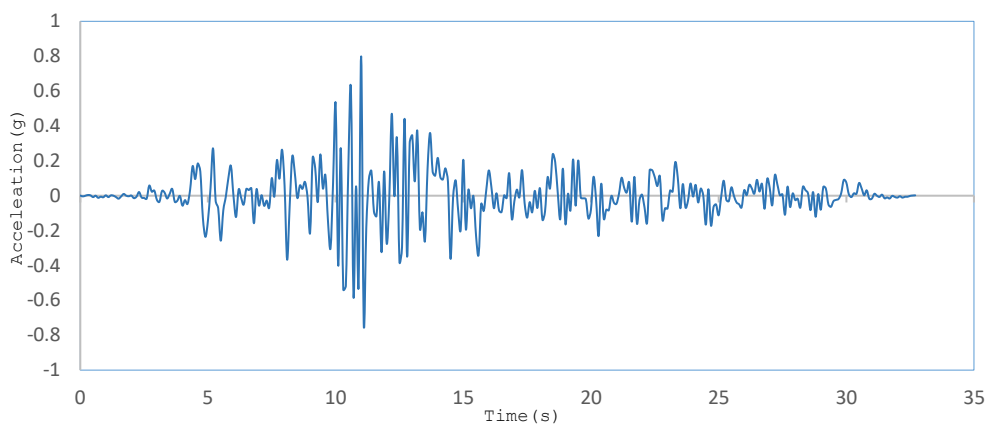


Figure 3. Accelerometer used in dynamic analysis of Azadi Dam (Tabas earthquake)

3. RESULTS AND DISCUSSION

3.1. ANALYSIS OF STRESS AND STRAIN OF AZADI DAM IN STEADY-STATE

The finite element analysis of Azadi Dam's body was performed after completing the construction phase and for steady-state conditions using Abaqus software. The model used in this analysis is Mohr-Columb elastoplastic, and the

analysis is performed according to the parametric conditions of total stress. Also, the mechanical properties of Azadi Dam materials used in the modeling are shown in Table 2.

Table 2. Geo mechanical parameters of stress-strain analysis

Material parameters	Pressure coefficient (K ₀)	Poisson's ratio(ν)	Elastic modulus(E) (kN/m ²)	Friction angle (ϕ)	Cohesion(c) (kN/m ²)	Dry density(γ_d) (kN/m ³)
Core	0.72	0.42	27500	30	100	20.4
Filter	0.54	0.36	35000	32	0	21.2
Drain	0.52	0.34	45000	35	0	21.7
Shell	0.47	0.32	70000	38	0	21.8
Foundation	0.33	0.25	10 ⁻⁶ ×2.6	24	1080	25.3

Stress and strain modeling has been done by both quasi-static and dynamic methods in the full reservoir (steady-state). The quantities used in the analyzes are shown in

Table 3. The stress quantity is denoted by the symbol σ , and the strain quantity is denoted by the symbol γ .

Table 3. Symbol of stress and strain analysis committees of Azadi Dam in Abacus software

Direction	Sheet	Quantity
X	XZ	σ_{xx}
Y	XZ	σ_{xy}
Y	YZ	σ_{yy}
X	XZ	γ_{xx}
Y	XZ	γ_{xy}
Y	YZ	γ_{yy}

3.2. STRESS AND STRAIN ANALYSIS OF AZADI DAM BY THE QUASI-STATIC METHOD

The simplest analysis of the behavior of a structure in an earthquake is the quasi-static method. This method is more common and older than other methods of seismic analysis. The use of this method dates back to 1950. In fact, in this method, the effect of the

earthquake is considered statically in the analysis by applying forces that are obtained by multiplying the earthquake coefficients in the weight of the slippery mass along the horizon and vertical. [Figure 4](#) shows the stress contour by the quasi-static method.

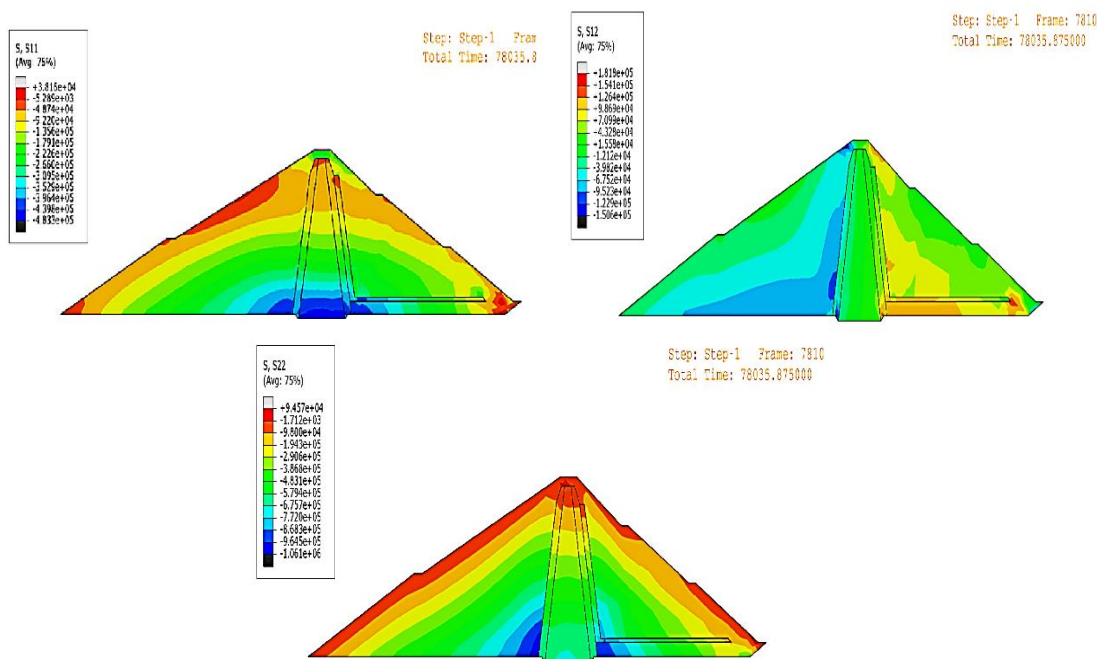
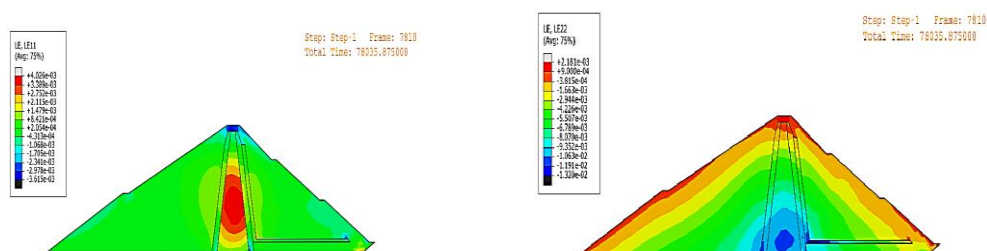


Figure 4. Distribution of Azadi dam stress in the quasi-static state in the direction of σ_{xx} , σ_{xy} and σ_{yy}

The results show that the highest stress in the σ_{xx} direction occurred due to the high adhesion of the clay and 483 kPa in the lower part of the core in the opposite direction of the X-axis. Also, the stress on both sides of the core (upstream and downstream shell) shows the value of 396 kPa, which is reduced by 18%, and as it moves away from the core, the amount of stress decreases to 135 kPa. The reduction of stress in this direction is due to heterogeneous materials. Most of the stress in the σ_{xy} state occurred in the upstream shell, which decreased by 32% with a certain geometric shape towards the upper levels. In this case, a lot of stress

concentration has occurred and requires special measures; this amount of stress concentration in the upper shell is 122 kPa and in the lower shell is 154 kPa. The highest stress in the σ_{yy} state of 964 kPa occurred in both the upstream and downstream shells near the core. In the core, the stress of 386 kPa is created, which shows a 61% reduction compared to the shell. The reduction of stress in the shell and core upwards is not the same and the speed of this reduction in the core is higher than the shell. The strain contour of the Azadi dam in the quasi-static method is shown in [Figure 5](#).



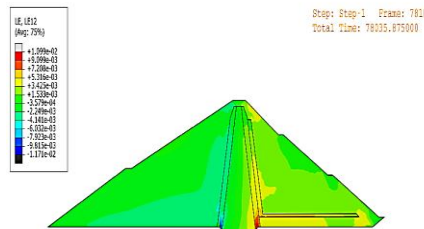


Figure 5. Distribution of Azadi dam strain in the quasi-static state in the direction of γ_{xx} , γ_{xy} and γ_{yy}

According to [Figure 5](#), the greatest strain occurred in the γ_{xx} direction inside the core. The maximum strain in the core is due to fine-grained materials with low permeability, the value of which is equal to 0.0034, which increases towards the shell and reaches the value of 0.0002 on the embankment slope. The strain irregularity is greater in the γ_{xy} direction, due to the multiple behaviors of the heterogeneous materials of the

dam, in this case, the maximum amount of strain in the core is 0.009 and the lowest amount of strain in the shell is 0.0015. The maximum strain in the γ_{yy} direction at the bottom of the core is 0.00132. The decrease in strain value of the γ_{xx} state is greater than the two states γ_{xx} and γ_{xx} . The reason for this behavior is the resistance of different parts of the heterogeneous dam.

3.3. DYNAMIC STRESS AND STRAIN ANALYSIS OF AZADI DAM

Dynamic analysis is the performance of numerical analysis on the body model and, if necessary, the foundation of the dam, which examines the behavior of the dam during the application of periodic seismic loads

and possible events after the earthquake by considering its behavior-strain of materials. The stress contour of the Azadi Dam is shown dynamically in [Figure 6](#).

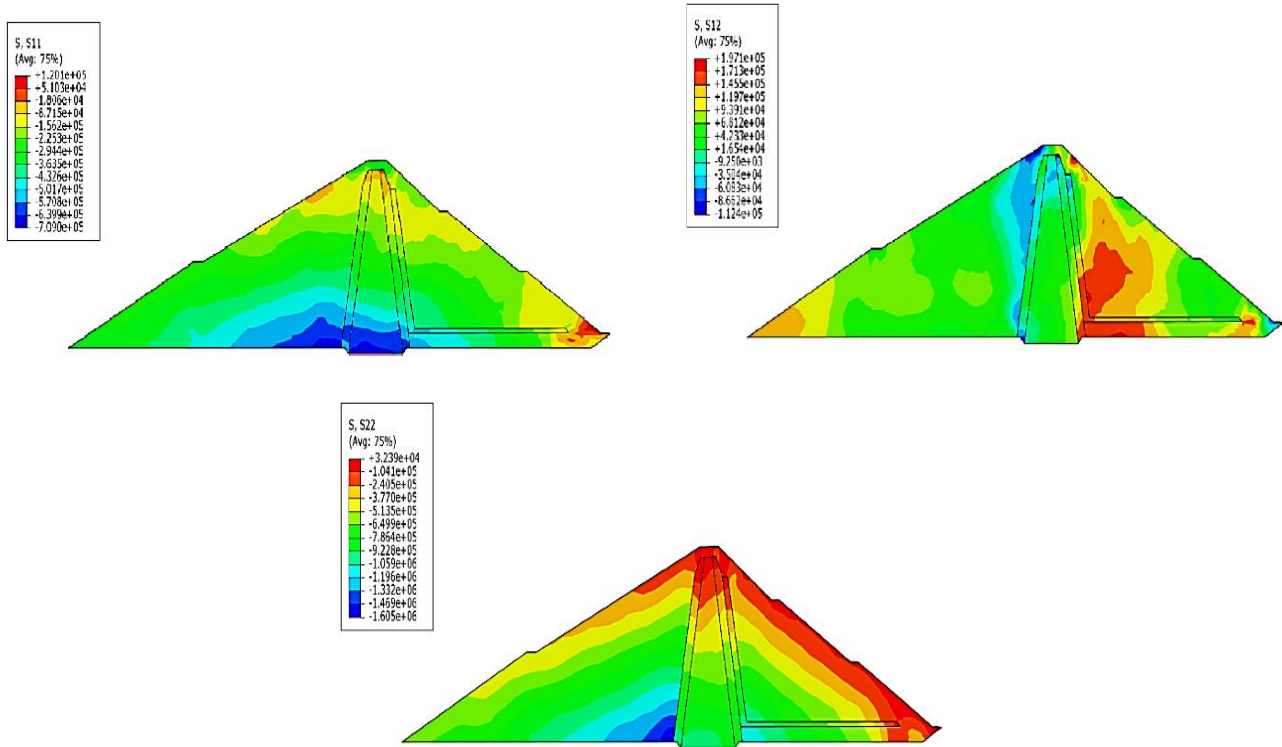


Figure 6. Distribution of Azadi dam stress in the dynamic state in the direction of σ_{xx} , σ_{xy} and σ_{yy}

The maximum amount of stress in the σ_{xx} direction after the seismic force in the core floor continues up to 30% of the shell width; this value is 502 kPa in the core and 640 kPa in the shell, due to the coarse-grained materials of the dam shell and high hardness. This is the part. The amount of stress in the upstream and downstream shells increases towards the upper levels, decreasing at the point of collision with the core relative to the shell. The stress in the σ_{xy} direction occurs in the lower shell and 20% at the lower level of the core, which is between 171-145 kPa. Most stress changes in this condition occur in the lower shell due to the phreatic line in this area. The core, in this

case, has almost regular stress of 42 kPa. The highest stress in the σ_{yy} direction occurs after the earthquake load is applied to the upstream shell, 15% away from the core, which is 1330 kPa. At the upper levels of the core at an angle of about 45° , the amount of stress is reduced so that in the middle of the shell will reach 650 kPa. Also, the stress in the lower shell and at the lower levels is the highest and decreases upwards. Its decreasing speed is higher than the upstream shell; the highest amount of stress in this part is 1059 kPa and in the middle of the shell is equal to 250 kPa. The strain contours of Azadi Dam are shown dynamically in [Figure 7](#).

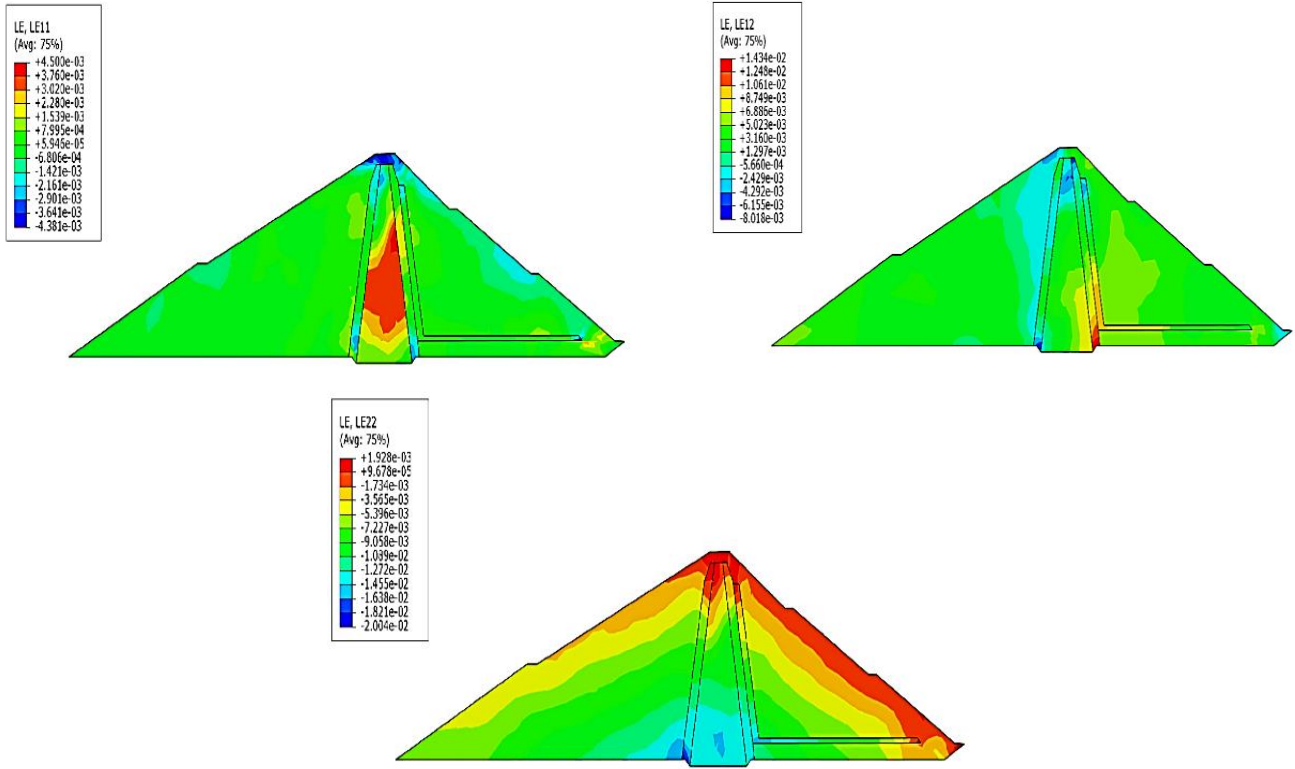


Figure 7. Distribution of Azadi dam strain in the quasi-static state in the direction of γ_{xx} , γ_{xy} and γ_{yy}

In the case of strain in the direction of γ_{xx} , due to the fineness of the materials in this area and their high density, the highest strain occurred in the core after the earthquake, with the highest strain in this area being 0.0037 and the lowest strain being 0.0007. The strain, in this case, is almost the same in all upstream shells and is equal to 0.0015, and the reason is the greater resistance of shell materials in this case. In the strain mode in the γ_{xy} direction, the maximum strain occurs as 0.0124 next to the core, then decreases to the inside of the core and reaches

the value of 0.003. In the upstream shell, the strain is approximately equal to 0.0011. The maximum strain occurs in the γ_{yy} direction at a distance of 0.125 of the width of the upstream shell next to the core and its value is approximately 0.016 and decreases with an angle of approximately 30 degrees to the higher level and reaches 0.007 at the middle. The maximum strain in the core is 0.014, which has decreased upwards. Three levels 1255m, 1275m, and 1300m are used for shell stress diagrams (Figure 8).

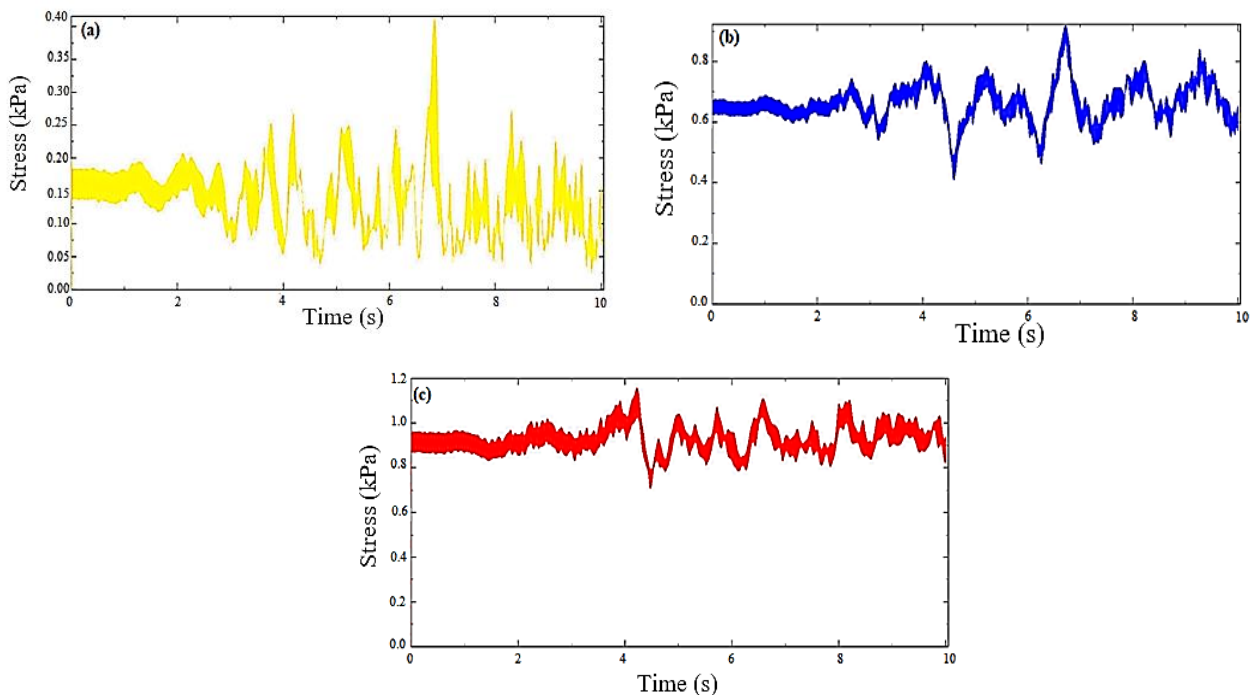


Figure 8. Stress curve at different levels of Azadi Dam shell a) EL. 1300 m, b) EL. 1275 m and c) EL. 1255 m

The interpretation of [Figure 7](#) is shown in [Table 4](#).

Table 4. Stress values at different levels of Azadi Dam shell

Specific frequency stress (kPa)	Frequency uniformity time (sec)	Minimum stress (kPa)	Minimum time(sec)	Maximum stress (kPa)	Maximum time(sec)	Level (masl)
850-950	3.5	710	4.35	1170	4.1	1300
610-640	2.14	413	4.6	910	6.6	1275
145-190	1.8	50	9.8	410	6.8	1255

According to [Table 4](#), the highest stress occurs on the floor, which is 29% higher than the middle level and almost 2 times (1.85) compared to the upper level of the dam. The minimum stress value will be 72% higher than the middle and 4 times higher than the upper level. It

should be noted that in the first few seconds of an earthquake, the dam with a certain frequency (which is related to acceleration) shows resistance. Stress analysis in all three directions σ_{yy} , σ_{xy} , and σ_{xx} in the core is investigated ([Figures 10, 9, and 11](#)).

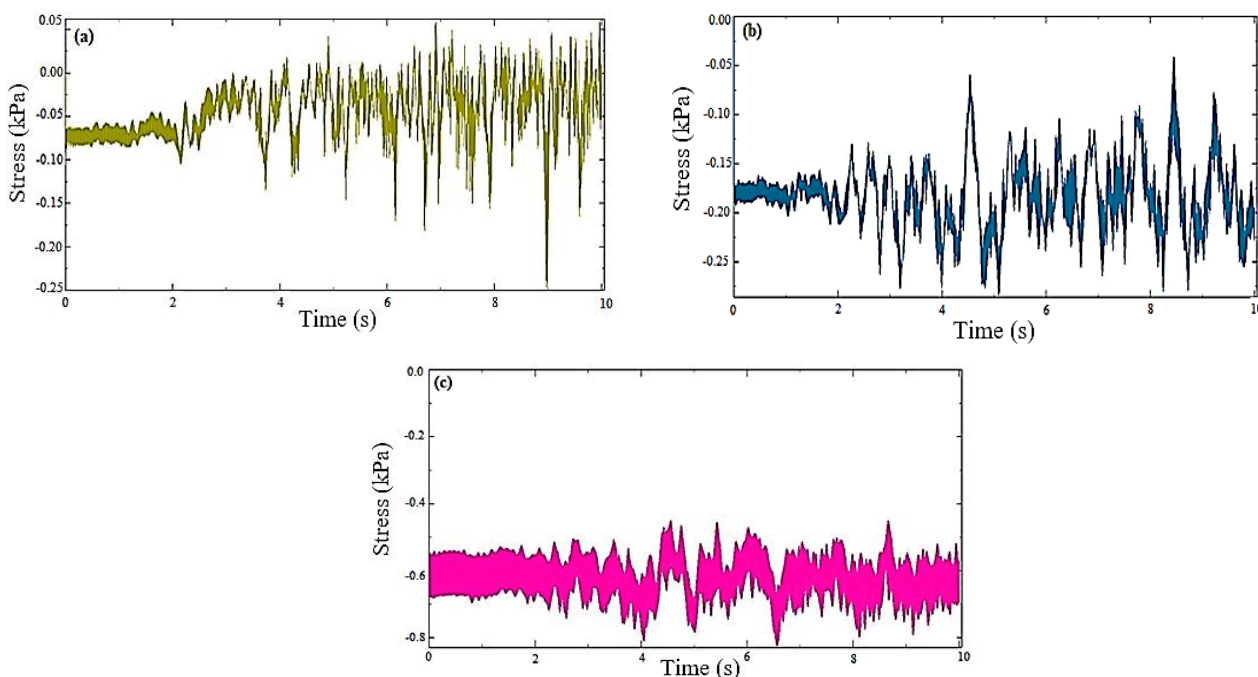


Figure 9. Stress curve in σ_{xx} direction at different levels of Azadi Dam core a) EL. 1300 m, b) EL. 1275 m and c) EL. 1255 m

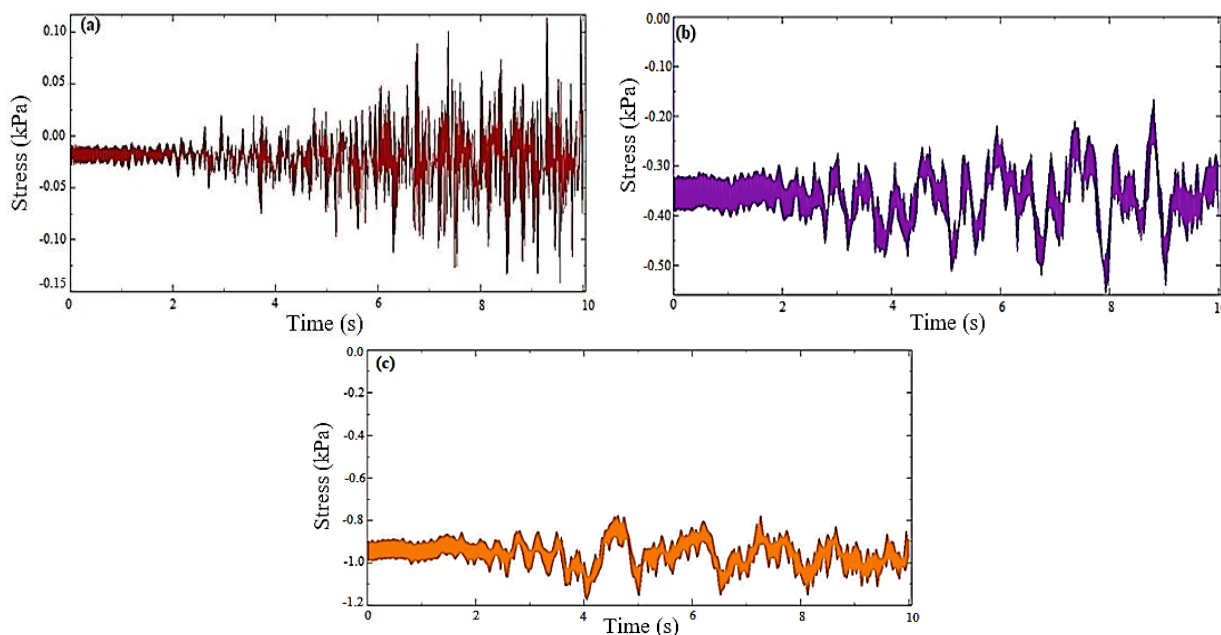


Figure 10. Stress curve in σ_{yy} direction at different levels of Azadi Dam core a) EL. 1300 m, b) EL. 1275 m and c) EL. 1255 m

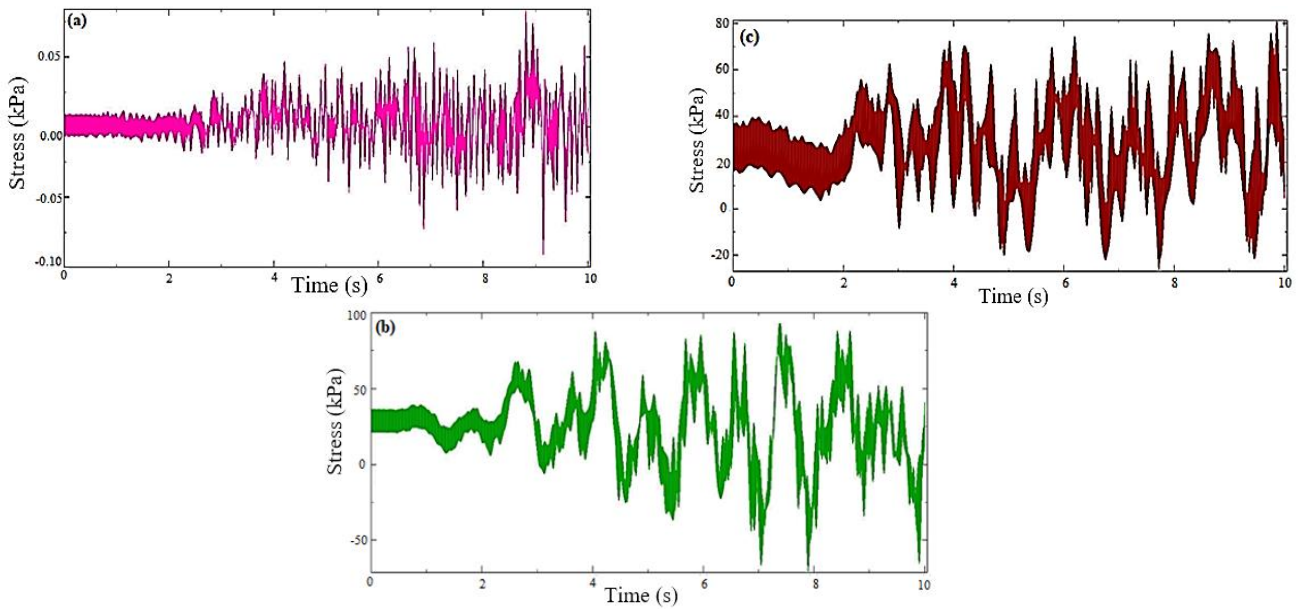


Figure 11. Stress curve in σ_{xy} direction at different levels of Azadi Dam core a) EL. 1300 m, b) EL. 1275 m and c) EL. 1255 m

The interpretation of [Figures 9,10 and 11](#) is shown in [Table 5](#).

Table 5. Stress values at different levels of Azadi dam core in the direction of σ_{yy} and σ_{xy} , σ_{xx}

σ_{yy} (kPa)	Stress time(sec)	σ_{xy} (kPa)	Stress time(sec)	σ_{xx} (kPa)	Stress time(sec)	Level (masl)
1100	4.1	81	9.8	830	6.7	1300
530	8	58	7.9	270	9	1275
225	9.4	54	9.1	120	9.2	1255

As we expected, the maximum stress of the Azadi Dam core during the earthquake in all cases fell to low levels. The highest core stress is related to the σ_{yy} direction, which is 46% higher in the bottom, 49% in the middle, and 49% higher than the other directions. In all cases, the stresses increase and decrease with a limited frequency for

approximately 2.5 seconds, after which the stress values will reach their minimum and maximum with a relatively high slope. Strain diagrams are shown in [Figures 12](#) to 14 in all three directions γ_{yy} , γ_{xy} and γ_{xx} at the core of the Azadi Dam.

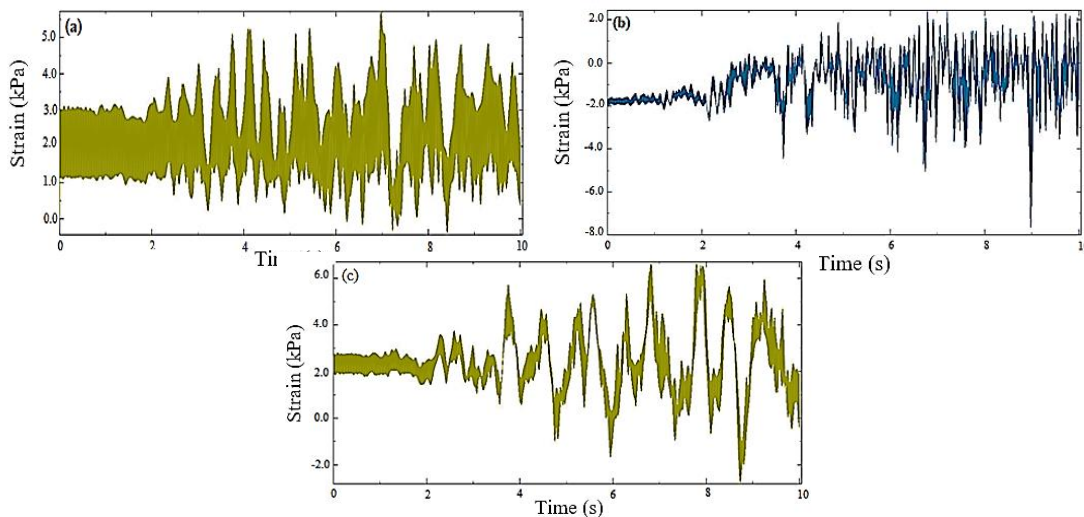


Figure 12. Strain curve in γ_{xx} direction at different levels of Azadi dam core a) EL. 1300 m, b) EL. 1275 m and c) EL. 1255 m

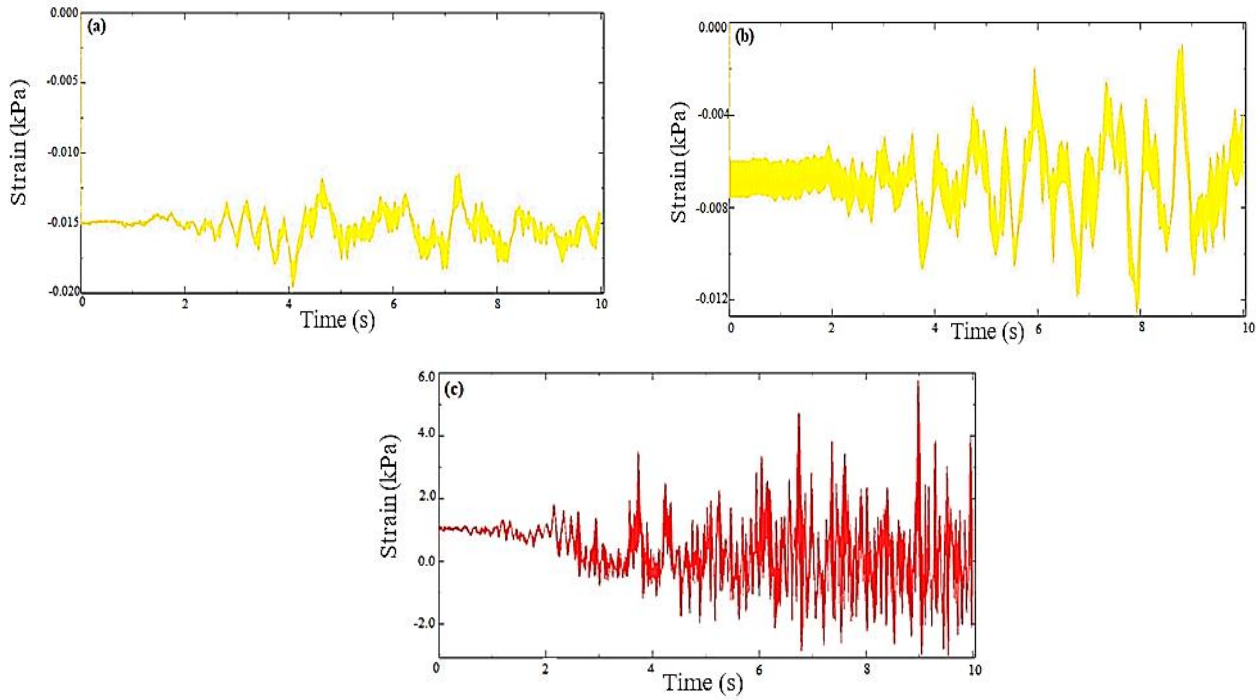


Figure 13. Strain curve in γ_{yy} direction at different levels of Azadi dam core a) EL. 1300 m, b) EL. 1275 m and c) EL. 1255 m

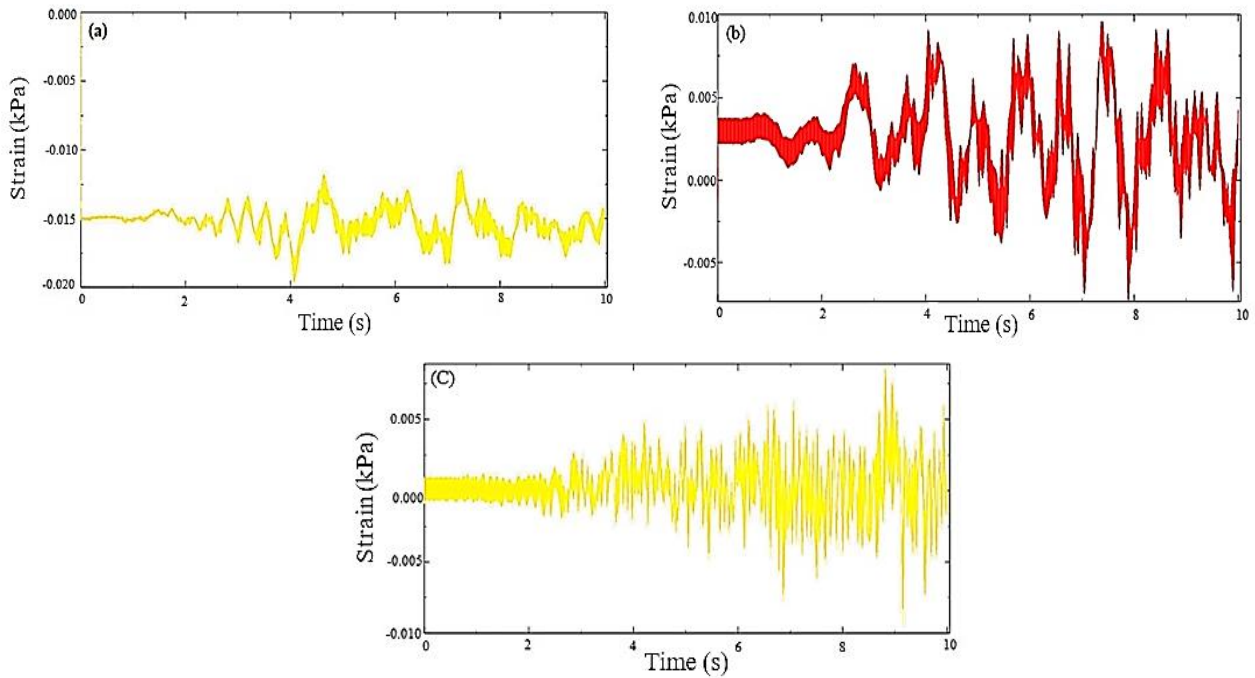


Figure 14. Strain curve in γ_{xy} direction at different levels of Azadi dam core a) EL. 1300 m, b) EL. 1275 m and c) EL. 1255 m

The interpretation of [Figures 12,13 and 14](#) is shown in [Table 6](#).

Table 6. Strain values at different levels of Azadi dam core in the direction of γ_{yy} and γ_{xy} , γ_{xx}

γ_{yy} (kPa)	Strain time(sec) γ_{yy}	γ_{xy} (kPa)	Strain time(sec) γ_{xy}	γ_{xx} (kPa)	Strain time(sec) γ_{xx}	Level (masl)
0.0028	9.2	0.00021	8.8	0.0025	9	1300
0.0057	7.5	0.012	7.8	0.005	8.5	1275
0.01	4.4	0.02	4.1	0.053	7	1255

The most strain occurs in the γ_{xy} direction and at high altitudes, almost twice as much as in other directions.

4. CONCLUSION

To control and prevent the increase of stresses during an earthquake, coarser-grained materials should be used in the body of the earth dam. The stress in the dynamic state is 49% higher in the σ_{xx} direction, in the σ_{xy} 30% direction, and in the σ_{yy} 28% direction than in the quasi-static state. At the 1255m level, the maximum shell stress is 29%, at the 1275m level 68%, and at the 1300 m level 72% more

than the core. In the case of strain in the direction of γ_{xx} , as expected, the highest strain occurs in the core due to the fine-grained materials in this area and their high density in the event of an earthquake. The maximum value of strain in this core of Azadi Dam is 0.0037, and the lowest value is 0.0007.

FUNDING/SUPPORT

Not mentioned any Funding/Support by authors.

ACKNOWLEDGMENT

Not mentioned by authors.

AUTHORS CONTRIBUTION

This work was carried out in collaboration among all authors.

CONFLICT OF INTEREST

The author (s) declared no potential conflicts of interests with respect to the authorship and/or publication of this paper.

5. REFERENCES

- [1] Ambraseys NN, Sarma SK. The response of earth dams to strong earthquakes. *Geotechnique*. 1967 Sep;17(3):181-213. [\[View at Google Scholar\]](#); [\[View at Publisher\]](#)
- [2] Sarma SK. Seismic stability of earth dams and embankments. *Geotechnique*. 1975 Dec;25(4):743-61. [\[View at Google Scholar\]](#); [\[View at Publisher\]](#)
- [3] Wang ZL, Makdisi FI, Egan J. Practical applications of a nonlinear approach to analysis of earthquake-induced liquefaction and deformation of earth structures. *Soil Dynamics and Earthquake Engineering*. 2006 Feb 1;26(2-4):231-52. [\[View at Google Scholar\]](#); [\[View at Publisher\]](#)
- [4] Tsai PH, Hsu SC, Lai J. Effects of core on dynamic responses of earth dam. In *Slope Stability, Retaining Walls, and Foundations: Selected Papers from the 2009 GeoHunan International Conference 2009* (pp. 8-13). [\[View at Google Scholar\]](#); [\[View at Publisher\]](#)
- [5] Tsompanakis Y, Lagaros ND, Psarropoulos PN, Georgopoulos EC. Simulating the seismic response of embankments via artificial neural networks. *Advances in Engineering Software*. 2009 Aug 1;40(8):640-51. [\[View at Google Scholar\]](#); [\[View at Publisher\]](#)
- [6] Elia G, Amorosi A, Chan AH, Kavvadas MJ. Numerical prediction of the dynamic behavior of two earth dams in Italy using a fully coupled nonlinear approach. *International Journal of Geomechanics*. 2011 Dec 1;11(6):504-18. [\[View at Google Scholar\]](#); [\[View at Publisher\]](#)
- [7] Mukherjee S. Seismic slope stability analysis of earth dam: Some modern practices. *Int. J. Recent Adv. Mech. Eng*. 2013;2(1):41-50. [\[View at Google Scholar\]](#); [\[View at Publisher\]](#)
- [8] Huang LJ, Sheen YN, Hsiao DH, Le DH. Numerical Analysis of Excavation Backfilled with Soil-based Controlled Low-Strength Materials: Part I-Static Analysis. *IJETAE*. 2014 Dec;4(12):132-9. [\[View at Google Scholar\]](#); [\[View at Publisher\]](#)
- [9] Panulinová E, Harabinová S. Methods for analyzing the stability of an earthen dam slope. In *Advanced Materials Research 2014* (Vol. 969, pp. 245-248). Trans Tech Publications Ltd. [\[View at Google Scholar\]](#); [\[View at Publisher\]](#)
- [10] Bandini V, Biondi G, Cascone E, Rampello S. A GLE-based model for seismic displacement analysis of slopes including strength degradation and geometry rearrangement. *Soil Dynamics and Earthquake Engineering*. 2015 Apr 1;71:128-42. [\[View at Google Scholar\]](#); [\[View at Publisher\]](#)
- [11] Zienkiewicz OC, Taylor RL, Nithiarasu P, Zhu JZ. *The finite element method*. London: McGraw-hill; 1977. [\[View at Google Scholar\]](#); [\[View at Publisher\]](#)
- [12] Mazaheri AR, Zeinolebadi Rozbahani M, Beiranvand B. Quasi-Static and Dynamic Analysis of Vertical and Horizontal Displacements in Earth Dams (Case Study: Azadi Earth Dam). *Journal of civil Engineering and Materials Application*. 2020 Dec 1;4(4):223-32. [\[View at Google Scholar\]](#); [\[View at Publisher\]](#)
- [13] ABAQUS Theory Manual, version 6.11-3., 2011. Dassault Systems. [\[View at Publisher\]](#)